THE JOURNAL OF BIOLOGICAL CHEMISTRY
Vol. 274, No. 29, Issue of July 16, pp. 20133–20138, 1999

Printed in U.S.A.

Disturbed Communication between Actin- and Nucleotide-binding Sites in a Myosin II with Truncated 50/20-kDa Junction*

(Received for publication, December 28, 1998, and in revised form, March 19, 1999)

Menno L. W. Knetsch‡, Taro Q. P. Uyeda§, and Dietmar J. Manstein¶

From the Department of Biophysics, Max Planck Institute for Medical Research, Jahnstrasse 29, D-69120 Heidelberg, Germany and §Bionic Design Group, National Institute for Advanced Interdisciplinary Research, 1-1-4 Higashi, Tsukuba, Ibaraki 305, Japan

The kinetic and functional consequences of deleting nine residues from an actin-binding surface loop (loop 2) were examined to investigate the role of this region in myosin function. The nucleotide binding properties of myosin were not altered by the deletion. However, the deletion affected actin binding and the communication between the actin- and nucleotide-binding sites. The affinity of M765NL for actin (644 nM) was approximately 100-fold lower than that of wild-type construct M765 (5.8 nM). Despite this reduction in affinity, actin binding weakened the affinity of ADP for the motor to a similar extent for both mutant and wild-type constructs. The addition of 0.5 μM actin decreased ADP affinity from 0.6 to 34 μM for M765NL and from 1.6 to 39 μM for M765. In contrast, communication between the actin- and nucleotide-binding sites appears disturbed in regard to phosphate release: thus, basal ATPase activity for M765NL (0.19 s^{-1}) was 3-fold larger than for M765 (0.06 s^{-1}), and the stimulation of ATPase activity by actin was 5-fold lower for M765NL. These results indicate different paths of communication between the actin- and nucleotide-binding sites, in regard to ADP and P_i release, and they confirm that loop 2 is involved in high affinity actin binding.

Myosins form a superfamily of ATP-driven molecular motors that produce unidirectional movement along actin filaments. Myosins consist of a globular catalytic domain, an extended neck region, and a functionally diverse tail region. The globular motor domain contains both actin- and nucleotide-binding sites. Force and movement are produced by this generic motor domain upon actin-induced ATP hydrolysis and subsequent product release (1, 2). The neck region contains one or more binding sites for calmodulin-like light chains. A rigid elongated structure is formed by the neck region; this amplifies small conformational changes in the globular motor domain, thus producing force and movement along actin filaments in steps of approximately 5–10 nm/ATP hydrolyzed (3, 4). The myosin II fragment, consisting of the motor domain and the neck region, is frequently referred to as subfragment-1 or S1. The functionally diverse tail region is important for formation of ordered assemblies or attachment to specific binding partners. This region of myosin II is for example involved in the formation of thick filaments in muscle (5–7) and in vesicle attachment in the case of myosin I and myosin V (6, 8–10).

Two prominent trypsin-sensitive surface loops form the borders of the 25-, 50-, and 20-kDa subdomains of S1 (11, 12). The first loop, loop 1, spanning the 25/50-kDa junction is situated near the nucleotide-binding site and is involved in determining the rate of ADP release (13, 14). The 50/20-kDa junction, also called loop 2, plays a central role in actin binding and consequently in tuning of the motor activity (15–17).

Myosin binding to actin has been described in a three-state model (18). First a collision complex is formed; this process involves long range electrostatic interactions. The resulting attached (*A*) state is a low affinity complex that undergoes a conformational change into the high affinity rigor (*R*) state. The equilibrium between the *A* and *R* states is strongly influenced by the nucleotide bound to the myosin motor. Myosin dissociates from actin upon ATP binding. After ATP hydrolysis, rebinding to actin and product release, the high affinity complex (*R*) is reformed, and simultaneously myosin moves one step forward along the actin filament.

The importance of loop 2 in tuning the enzymatic activity of myosin II was demonstrated in studies in which the native loop 2 was replaced with that from other myosins. Insertion of β-cardiac or skeletal loop 2 in smooth muscle heavy meromyosin led to an unregulated heavy meromyosin (16).

Replacement of *Dictyostelium* myosin loop 2 with several other loop 2 regions resulted in chimeric myosins with actin-activated ATPase activities that correlated well with the activity of the donor myosins (15). Insertion of positive charges into *Dictyostelium* myosin loop 2 increased the affinity for actin in the absence and presence of Mg^{2+}-ATP. These constructs displayed a 2–3-fold increase in k_{cat}, a more than 10-fold reduction in K_{app} for actin, and an up to 70-fold increase in catalytic efficiency (17).

Up to now all mutational analyses of loop 2 involved enlarging of this region. From the atomic structure of the *Dictyostelium* myosin motor domain, it appears that a minimal size of the loop spanning the 50/20-kDa junction may be required to retain correct communication between the actin- and nucleotide-binding sites (3). Shortening of loop 2 is expected to produce conformational stress and a slight distortion of the myosin motor domain. To test the effect of loop 2 shortening on myosin motor activity, we have now constructed and characterized a *Dictyostelium* myosin II that has 9 amino acids of this loop exchanged for a single valine residue. ATPase rates, actin binding characteristics, nucleotide binding, *in vitro* motility, and functional complementation *in vivo* of this mutant myosin were studied to gain a better understanding of the role of loop 2 in myosin motor function.

* The work was supported by the Max Planck Society (Germany). The costs of publication of this article were defrayed in part by the payment of page charges. This article must therefore be hereby marked "*advertisement*" in accordance with 18 U.S.C. Section 1734 solely to indicate this fact.

‡ Supported by a long term fellowship from the European Molecular Biology Organization.

¶ To whom correspondence should be addressed: Max-Planck-Institut für Medizinische Forschung, Jahnstrasse 29, D-69120 Heidelberg, Germany. Tel.: 49-6221-486-212; Fax: 49-6221-486-437; E-mail: manstein@mpimf-heidelberg.mpg.de.

EXPERIMENTAL PROCEDURES

Proteins and Reagents—Rabbit skeletal actin was prepared by the method described by Lehrer and Kerwar (19). Mant-ATP was synthesized using the protocol described by Hiratsuka (20). (4′-(iodoacetamido)anilino)naphthalene-6-sulfonic acid used to label actin with a fluorescent pyrene group (21) was from Molecular Probes. G418 was from Life Technologies, Inc., imidazole from BDH Laboratory Supplies (Poole, United Kingdom). All other chemicals were purchased from Sigma.

Plasmid Construction—Subcloning was done using standard procedures (22). The vector pBIGMyD containing the complete coding sequence of the *Dictyostelium* myosin heavy chain A was used to construct the loop 2 deletion mutant, NL-myosin. First the native loop 2 sequence TTCAATGATCCAAACATTGCCAGTGGTGCAAAG, encoding FNDPNIASRAK, was changed using oligo-directed mutagenesis into TTCGAATCTAGACTTAAG, encoding FESRLK. This gene was digested with *Bst*B I and *Afl*III, filled in using DNA polymerase I Klenow fragment and self-ligated. The resulting sequence was TTCGTTAAG encoding FVK. Thus residues 613 to 621 were exchanged for a single valine residue. Plasmid pDH20, a pDXA-3H derivative, was used for the expression of M765 under the control of the *Dictyostelium* actin 15 promoter (23). M765 includes the first 765 amino acids of the *Dictyostelium mhcA* gene and carries a C-terminal His-7 tag. The NL-mutation was transferred to M765 from the plasmid encoding NL-myosin. The resulting plasmid pDH21 encodes M765NL.

Protein Purification—Dictyostelium cells were grown on HL-5 medium supplemented with 10 μg/ml G418 (24). Cells were harvested when a density of $4-6 \times 10^6$ was reached. Typically 30–40 g of cells were used per purification, yielding up to 2 mg of pure protein per gram of cells (wet weight). The protein purification was performed as described earlier (25). Briefly, cells were Triton-lysed in the presence of alkaline phosphatase. The expressed myosin was extracted with Mg-ATP from the Triton-insoluble pellet. The His-tagged myosin head fragment (MHF)[1] was purified by Ni^{2+} affinity chromatography. Full-length myosin and NL-myosin were purified as described by Ruppel *et al.* (26).

Stopped Flow Experiments—Stopped flow experiments were performed at 20 °C with a Hi-tech Scientific SF61 stopped-flow spectrophotometer equipped with a 100 W Xe/Hg lamp and a monochromator. The mant-derivatives of ATP or ADP were excited at 364 nm, pyrene was excited at 365 nm, and the emitted light was detected after passing through a KV389-nm cut-off filter. The rate of MHF binding to pyrene-actin was monitored by the change in light scattering at 410 nm and detected at an angle of 90° to the incident light. Data were stored and analyzed using software provided by Hi-tech. Transients were determined as the average of three to five consecutive shots of the stopped-flow machine. All concentrations refer to the concentration of the reactants after mixing in the stopped-flow observation cell. The experimental buffer was 20 mM MOPS, pH 7.0, 5 mM $MgCl_2$, 100 mM KCl.

Transient Kinetic Properties of Myosin Head Fragments—Dictyostelium MHFs have been shown to follow the same basic mechanism of actin and nucleotide binding that was described for S1 from rabbit fast skeletal muscle myosin and other muscle myosins. The dynamics of ATP binding and hydrolysis by the MHFs were analyzed in terms of the model shown in Scheme 1 (27) in which M represents *Dictyostelium* MHF. In this and the following schemes a notation is used that distinguishes between the constants in the presence and absence of actin by using bold ($\mathbf{k}_{+1}$, $\mathbf{K}_1$) *versus* italics type (k_{+1}, K_1); subscript A and D refer to actin ($\mathbf{K}_A$) and ADP (K_D), respectively.

$$M + ATP \underset{k_{-1}}{\overset{k_{+1}}{\rightleftharpoons}} M \cdot ATP \underset{k_{-2}}{\overset{k_{+2}}{\rightleftharpoons}} M \cdot \underset{k_{-3}}{\overset{k_{+3}}{ATP}} \; M \cdot ADP \cdot P_i$$

SCHEME I

Acto-myosin complexes dissociate upon binding of ATP. This dissociation and the effect of ADP on it were analyzed in terms of models developed by Millar and Geeves (28) and Siemanowski and White (29). A and M in Scheme 2 represent actin and MHF, respectively.

$$A \cdot M + ATP \overset{\mathbf{K}_1}{\rightleftharpoons} A \cdot M \cdot ATP \overset{\mathbf{k}_{+2}}{\longrightarrow} A + M \cdot ATP$$

$$A \cdot M \cdot ADP \overset{\mathbf{K}_{AD}}{\rightleftharpoons} A \cdot M + ADP$$

SCHEME II

After mixing A·M and ATP a rapid equilibrium is reached, defined by the equilibrium constant $\mathbf{K}_1$. The following isomerization of the ternary complex limits the maximum rate of actin dissociation from the complex. Thus the observed rate constant for the ATP-induced dissociation of actin is given by Eq. 1.

$$k_{obs} = [ATP]\mathbf{K}_1\mathbf{k}_{+2}/(1 + \mathbf{K}_1[ATP]) \quad \text{(Eq. 1)}$$

where $\mathbf{K}_1$ represents the association constant for the ternary complex formation. In the presence of ADP, the two nucleotides compete for binding to A·M. Assuming a rapid equilibrium between A·M and the ADP bound state, k_{obs} for a fixed ATP concentration is given by Eq. 2.

$$k_{obs} = k_0/(1 + [ADP]/\mathbf{K}_{AD}) \quad \text{(Eq. 2)}$$

where the k_{obs} in the absence of ADP is k_0 and the dissociation constant $\mathbf{K}_{AD}$ represents the affinity of ADP for the acto-myosin complex (29).

Binding of *Dictyostelium* myosin to actin is discussed in terms of the three-state docking model originally formulated for skeletal muscle myosin (18) (Scheme 3).

$$A + M(\cdot N) \overset{\mathbf{K}_0}{\quad} A \sim M(\cdot N) \overset{\mathbf{K}_1}{\rightleftharpoons} A{-}M(\cdot N) \overset{\mathbf{K}_2}{\rightleftharpoons} A \cdot M(\cdot N)$$

Collision complex *A state* *R state*

SCHEME III

Determination of ATPase Activity—ATPase activity was measured as described (30). The liberated phosphate was quantified using the colorimetric assay described by White (31).

RESULTS

Wild-type and mutant myosin constructs were expressed at similar levels in *Dictyostelium discoideum*. Cells were lysed in the presence of alkaline phosphatase to remove all ATP, and co-sedimentation with actin was used as the first purification step of MHF. In the case of M765 more than 95% of total MHF precipitated with actin, whereas for M765NL approximately 35% was recovered in the Triton-insoluble pellet. Yields of approximately 3 and 1 mg of MHF/gram of cells were obtained for M765 and M765NL following Mg^{2+}-ATP extraction and Ni^{2+}-NTA chromatography. The purity of the myosin or MHFs was ≥95% as evaluated by Coomassie staining (data not shown). The M765 constructs were used for nucleotide- and actin binding studies as they are soluble under physiological salt conditions, whereas full-length myosin constructs were used for *in vitro* motility assays and *in vivo* rescue studies.

Binding of mant-ATP to M765 and M765NL resulted in similar changes in fluorescence intensity, and almost identical values of 9.2×10^5 M^{-1} s^{-1} and 8.9×10^5 M^{-1} s^{-1} for the second order rate constant for mant-ATP binding $\mathbf{K}_1\mathbf{k}_{+2}$ were obtained (Fig. 1*A* and Table I). The affinity of mant-ADP (K_D) for M765NL was increased 2.5-fold compared with M765 (0.61 and 1.56 μM, respectively). This increase was mainly because of a 2.5-fold reduction in the rate of mant-ADP dissociation (k_{-D}) from M765NL, 0.50 s^{-1} compared with 1.21 s^{-1} for M765. The second order rate constant for mant-ADP binding (k_{+D}) was virtually identical to that of M765. Values of 8.2×10^5 M^{-1} s^{-1} *versus* 7.8×10^5 M^{-1} s^{-1} were obtained for the mutant and wild-type construct, respectively (Fig. 1*B* and Table I).

Myosin-actin binding characteristics can be monitored by measuring the quenching that occurs when myosin binds pyrene-labeled actin (32). Fluorescence quenching is thought to occur when myosin undergoes a conformational change from the attached weakly bound *A*-state to the strongly bound rigor *R*-state (18). The actin binding parameters determined for wild-type construct M765 were similar to those obtained with an S1-like *Dictyostelium* myosin II construct (17, 27). In contrast, addition of M765NL to pyrene-actin did not produce any fluorescence quenching. Co-precipitation of actin and M765NL demonstrated that actin binding occurs, but much less effective than with wild-type M765. Addition of excess ATP completely

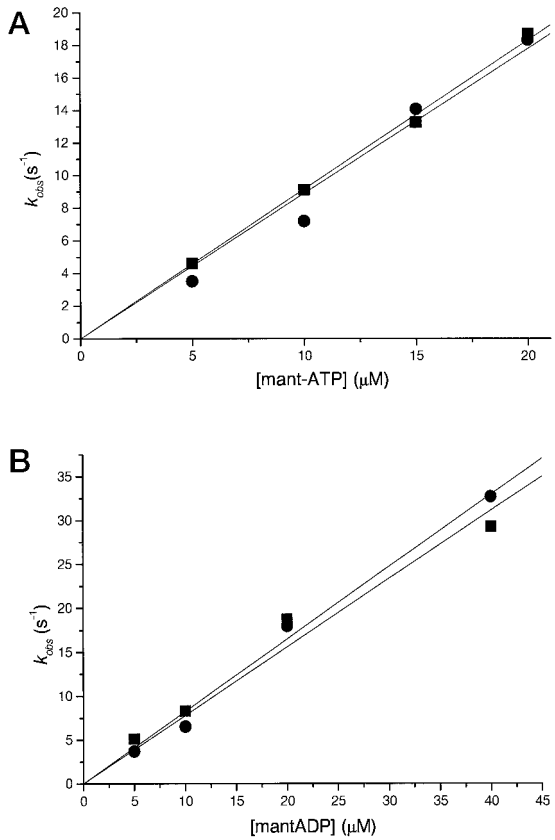

FIG. 1. **Binding of mant-ATP and mant-ADP to M765 and M765NL.** Myosin motor domains M765 (■) and M765NL (●) were incubated with increasing concentrations of mant-ATP (5, 10, 15, 20 μM) (*A*) or mant-ADP (5, 10, 20, 40 μM) (*B*). The fluorescence was excited at 364 nm, and the resulting curves were fitted to a single exponential. The observed rate constant k_{obs} are plotted against the mant-ATP or mant-ADP concentration.

released the bound M765NL from actin (data not shown).

The rate of actin binding to M765 and M765NL was measured by light scattering to confirm the reduced affinity of M765NL for actin. The time-dependent increase in light scattering that follows mixing of the myosin constructs with an excess of pyrene-actin could be described by a single exponential function. The k_{obs} values increased linearly with increasing concentrations of actin over the range from 0.5 to 2.5 μM for M765 and up to 10 μM actin in the case of M765NL (Fig. 2). The slopes of the lines define the second order rate constants, $\mathbf{k}_{+A}$, for actin binding (27). Values of $3.6 \pm 0.31 \times 10^6$ M^{-1} s^{-1} and $0.43 \pm 0.01 \times 10^6$ M^{-1} s^{-1} were obtained for M765 and M765NL, respectively. Because interaction of M765NL with pyrene-actin does not produce a change in the fluorescence signal, the rate of dissociation of the acto-myosin complex ($\mathbf{k}_{-A}$) was determined in a competition experiment. In this experiment acto-M765NL complex was mixed with increasing concentrations of M765 (5 to 40 μM) and quenching of pyrene-actin fluorescence upon binding of M765 was recorded. The recorded processes were clearly biphasic and could be fitted to a biexponential function. The first phase of the observed process represents the binding of M765 to noncomplexed pyrene-actin. The k_{obs} values for the fast phase increased with higher concentrations of M765 whereas the k_{obs} for the slow phase was 0.85 s^{-1} in the presence of 2 μM M765 and decreased to 0.3 s^{-1} at 10 μM M765 (Fig. 2*B*). This decrease in k_{obs} with increasing [M765] could be described by a hyperbola with a dissociation equilibrium constant $\mathbf{K}_A$ of approximately 490 nM. The rate constant for actin dissociation from M765NL ($\mathbf{k}_{-A}$) is defined by k_{min} (0.29 s^{-1}). A dissociation rate constant $\mathbf{k}_{-A}$ of 0.29 s^{-1} and an association rate constant $\mathbf{k}_{+A}$ of 0.45×10^6 M^{-1} s^{-1} predict a value for $\mathbf{K}_A$ of 644 nM (Table I). The corresponding values for M765 were determined as 0.02 s^{-1} for $\mathbf{k}_{-A}$ and 5.8 nM for $\mathbf{K}_A$ as described earlier (17).

To study the communication between nucleotide- and actin-binding sites of M765NL, we examined the ATP-induced dissociation of acto·MHF as described in Scheme II. Preformed acto·MHF complex was mixed with increasing concentrations of ATP and the decrease in light scattering was monitored as the complex dissociated. The observed rate constants were linearly dependent on ATP concentrations in the range up to 25 μM (Fig. 3*A*). The second order binding constant $\mathbf{K}_1\mathbf{k}_{+2}$ (see Scheme II) was increased 5-fold for M765NL to 5.1×10^5 M^{-1} s^{-1}. At higher concentrations of ATP (>1 mM) the observed rate constants saturate (Fig. 3*B*) and the [ATP] dependence of k_{obs} could be described by a hyperbola (Eq. 1) as predicted by Scheme II, where $k_{max} = \mathbf{k}_{+2}$ and $\mathbf{K}_{0.5} = 1/\mathbf{K}_1$. For M765NL both $\mathbf{K}_1$ and $\mathbf{k}_{+2}$ were increased compared with M765 (Table I).

The affinity of ADP for the pyrene-actin·MHF ($\mathbf{K}_{AD}$) was determined from the competitive inhibition of ATP-induced dissociation of acto·MHF as shown in Fig. 4. Again the decrease in light scattering was monitored. The resulting data were fitted to Eq. 2 as shown under "Experimental Procedures." Dissociation constants of 38 and 34 μM were obtained for M765 and M765NL, respectively (Table I).

Steady-state ATPase activity was measured for wild-type and mutant myosin constructs. First the high-salt Ca^{2+} ATPase rate was determined. Hydrolysis of ATP in the absence of Mg^{2+} but in the presence of Ca^{2+} and high concentrations of salt results in high hydrolysis rates, because these conditions favor the release of hydrolysis products (33). High salt-Ca^{2+} ATPase did not significantly differ for M765 and M765NL, indicating that the mutant does not have a defect in the mechanism of hydrolysis (Table II). M765NL and full-length NL-myosin showed elevated basal levels of Mg^{2+}-ATPase hydrolysis activity when compared with the wild-type constructs (Table II.). M765NL and NL-myosin showed little stimulation of their ATPase activity by actin. At concentrations much lower than K_{app}, the dependence of the apparent ATPase rate on actin concentration can be fitted to a straight line and the apparent second order rate constant k_{cat}/K_{app} of the reaction can be determined from the slope of this line. M765NL gave a 5–6-fold decreased value of 0.045×10^5 M^{-1} s^{-1} compared with M765 (0.23×10^5 M^{-1} s^{-1}), and the results suggest a more than 5-fold increase in K_{app} for M765NL (Fig. 5).

The deletion also affects the motor function of myosin. *In vitro* motility studies demonstrated that the NL-myosin binds actin, but all actin filaments diffused away instantly upon ATP addition (data not shown). Furthermore, NL-myosin did not interfere with motility of wild-type myosin when mixed in an *in vitro* motility experiment (data not shown). This behavior of NL-myosin in *in vitro* motility experiments can be explained by its low affinity for actin and high rate for ATP-induced dissociation of acto-M765NL (34). The deletion in the 50/20-kDa junction strongly affects myosin function *in vivo* also. *Dictyostelium* offers the unique possibility to assess myosin function *in vivo* (35, 36). *Dictyostelium* cells lacking the myosin II gene show a defined phenotype. Myosin II null cells are unable to grow in suspension culture, are often multinucleated, show a defect in the capping of cell surface receptors and cannot complete the developmental cycle (37, 38). Introduction of wild-type myosin in myosin II null cells completely rescues these phenotypic changes (35). When the NL-myosin was reintroduced into the myosin null cells, none of the developmental defects were rescued, and the transformants were not able to grow in sus-

TABLE I
Transient kinetic analysis
Experimental conditions for all measurements: 20 mM MOPS, 5 mM $MgCl_2$, 100 mM KCl, pH 7.0, 20 °C.

	Rate constant	M765	M765NL
Nucleotide binding to MHF	K_1k_{+2} ($M^{-1}s^{-1}$)	9.2 ± 0.13 × 10^5	8.9 ± 0.45 × 10^5
	k_{+D} ($M^{-1}s^{-1}$)	7.8 ± 0.49 × 10^5	8.2 ± 0.29 × 10^5
	k_{-D} (s^{-1})	1.21 ± 0.063	0.50 ± 0.021
	K_D (μM) (k_{-D}/k_{+D})	1.6 ± 0.13	0.61 ± 0.033
Nucleotide binding to acto · MHF	$\mathbf{K_1k_{+2}}$ ($M^{-1}s^{-1}$)	1.0 ± 0.10 × 10^5	5.1 ± 0.14 × 10^5
	$\mathbf{K_1}$ (M^{-1})	557	1029
	$\mathbf{k_{+2}}$ (s^{-1})	176	500
	$\mathbf{K_{AD}}$ (μM)	38.8 ± 6.68	34.0 ± 3.15
Actin binding to MHF	$\mathbf{k_{+A}}$ ($M^{-1}s^{-1}$)	3.4 ± 0.13 × 10^6	0.45 ± 0.01 × 10^6
	$\mathbf{k_{-A}}$ (s^{-1})	0.020 ± 0.0012	0.29 ± 0.029
	$\mathbf{K_A} = \mathbf{k_{-A}}/\mathbf{k_{+A}}$ (nM)	5.9 ± 0.41	644 ± 66.1

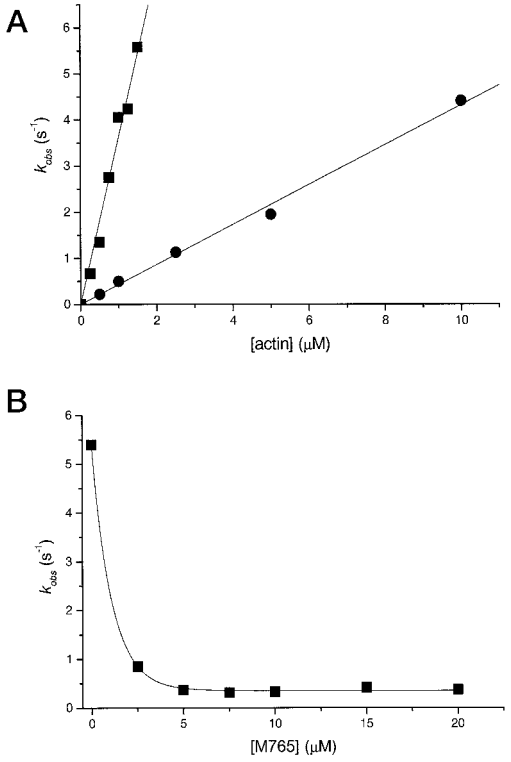

FIG. 2. **Actin binding characteristics of M765 and M765NL.** *A*, increasing concentrations of actin were incubated with 0.25 μM MHF. Light scattering of 410 nm light was collected at 90° incident angle. The resulting curves were fitted to a single exponential, and the k_{obs} was plotted against the actin concentration. The k_{obs} values increase linearly with increasing concentrations of actin. The slopes of the best-fit lines define second order rate constants $\mathbf{k_{+A}}$ of 3.6 ± 0.31 × 10^6 M^{-1} s^{-1} and 0.43 ± 0.17 × 10^6 M^{-1} s^{-1} for M765 (■) and M765NL (●), respectively. *B*, rate of dissociation of the acto-myosin complex ($\mathbf{k_{-A}}$). Increasing concentrations of M765 (5–40 μM) were mixed with acto-M765NL, and quenching of pyrene-actin fluorescence was recorded. The recorded processes were clearly biphasic and could be fitted to a bi-exponential function. The first phase of the observed process represents the binding of M765 to noncomplexed pyrene-actin. The k_{obs} values for the fast phase increased with higher concentrations of M765, whereas the k_{obs} for the slow phase was 0.85 s^{-1} in the presence of 2 μM M765 and decreased to 0.3 s^{-1} at 10 μM M765. This decrease in k_{obs} with increasing [M765] could be described by a hyperbola with a dissociation equilibrium constant $\mathbf{K_A}$ of approximately 490 nM. The rate constant for actin dissociation from M765NL ($\mathbf{k_{-A}}$) is defined by k_{min} (0.29 s^{-1}).

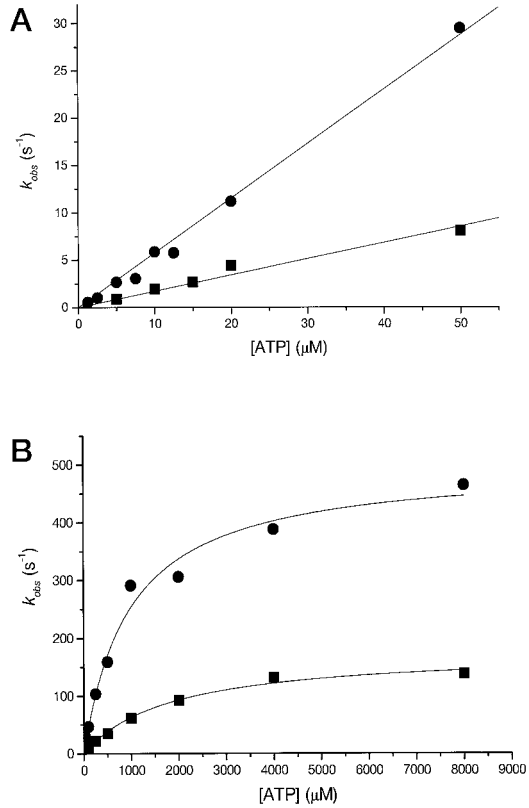

FIG. 3. **ATP induced dissociation of acto·MHF.** *A*, the decrease in light scattering observed upon mixing of 0.5 μM acto·M765 (■) or a 0.5 μM actin, 2.5 μM M765NL mixture (●) with increasing ATP concentrations were fitted to a single exponential. The resulting k_{obs} at low ATP concentrations (5–25 μM) are linearly dependent on [ATP]. *B*, at high concentrations of ATP (>2 mM) the observed rate constants saturate, and the [ATP] dependence of k_{obs} can be fitted by a hyperbola as predicted by Scheme II.

pension (data not shown). This indicates that NL-myosin is not functional *in vivo*.

DISCUSSION

In this report we describe the kinetic and functional analysis of myosin mutant constructs M765NL and NL-myosin, in which the 50/20-kDa junction is truncated. Previously we had examined the effect on myosin function of increasing the length and altering the charge of the loop 2 region and found that extensions of the loop 2 region by up to 20 residues did not alter kinetic behavior of the myosin motor. In contrast there was a clear correlation between the charge of loop 2, the activation by actin of the mutant constructs' ATPase rates and the strength of interaction of mutant motor domains and actin (17). Crystallographic studies of the myosin motor domain predict that a minimal size of loop 2 is required for normal motor function. The deletion of part of loop 2 should result in local structural perturbations that interfere with normal communication between the actin-binding site and other regions of the myosin motor (3, 4, 33).

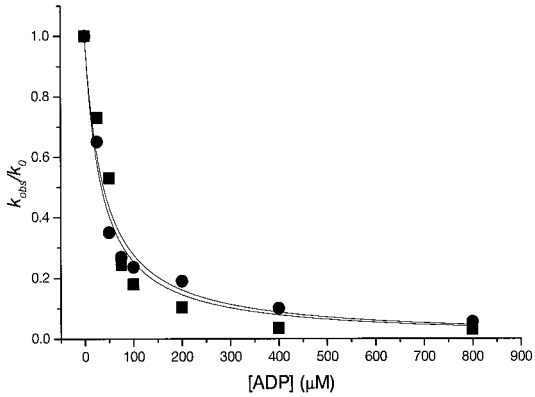

FIG. 4. **ADP inhibition of ATP induced dissociation of acto·MHF.** Preformed acto·M765 (■) or acto·M765NL (●) complexes (as in Fig. 3) with increasing amounts of ADP were mixed with saturating concentrations of ATP (400 μM). k_0 corresponds to k_{obs} in the absence of ADP. The ratio between k_{obs} and k_0 was plotted against [ADP] and fitted with Eq. 2 to determine the dissociation constant of ADP for acto·MHF.

TABLE II
Steady-state ATPase activities

Results for ATPase activity measurements are given as P_i liberated/myosin head/s. Reactions were performed as described under "Experimental Procedures" at 30 °C. MHF concentrations were 1 μM, and the concentration of myosin was 0.4 μM. Actin was used at a final concentration of 20 μM. The data presented are the mean of at least three independent measurements from at least two independent protein preparations.

	Mg^{2+} ATPase	Mg^{2+} ATPase + 20 μM actin	High salt Ca^{2+} ATPase
M765	0.06 ± 0.02	0.54 ± 0.03	1.45 ± 0.20
M765NL	0.19 ± 0.02	0.30 ± 0.03	1.33 ± 0.17
Wild-type-myosin	0.07 ± 0.05	0.78 ± 0.14	2.9 ± 0.5
NL-myosin	0.25 ± 0.07	0.29 ± 0.10	ND[a]

[a] ND, not determined.

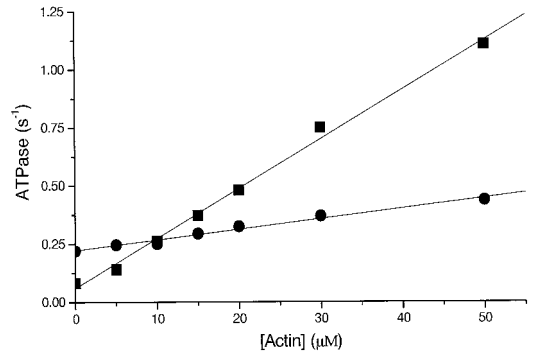

FIG. 5. **Actin stimulation of ATPase activity.** ATPase activities for M765 (■) and M765NL (●) were measured at different actin concentrations. The resulting activities were plotted against the actin concentration and fitted to a straight line.

The present transient kinetic analysis of M765NL demonstrates that nucleotide binding to MHF is not affected by partial deletion of loop 2. The affinities of M765NL for both mant-ATP and mant-ADP are very similar to the values determined for wild-type M765. The largest change observed with the mutant myosin was a 2.5-fold increase in ADP affinity.

In contrast to the interaction with nucleotide, the deletion in loop 2 had a large effect on the association and dissociation constants for actin binding, resulting in approximately 100-fold lower affinity for actin. Pyrene quenching was not observed with M765NL. It has been reported that quenching of pyrene-actin fluorescence by myosin occurs upon the conformational change leading to the formation of the actin bound *R*-state of myosin (18). Therefore, the lack of pyrene fluorescence quenching upon binding of M765NL to pyrene-labeled actin could result from the inability of the mutant myosin motor domain to complete the transition from the weakly bound, attached (*A*) state to the strongly bound (*R*) state. However, the nonformation of *R*-states is expected to result in a much higher reduction in affinity, and the kinetic data suggest that the partial loss of loop 2 has similar effects on both $\mathbf{k}_{+A}$ and $\mathbf{k}_{-A}$. Therefore, a change in affinity cannot be entirely attributed to a $\mathbf{K}_2$ effect, as $\mathbf{k}_{+A}$ and $\mathbf{k}_{-A}$ correspond to $\mathbf{K}_0\mathbf{k}_{+1}$ and $\mathbf{k}_{-1}/(1 + \mathbf{K}_2)$, respectively (see Scheme III). Additionally, if *R*-states cannot be formed, one would expect little acceleration of the M765NL ATPase rate and little weakening of ADP binding following the addition of actin.

We did indeed observe a similar change in ADP affinity upon addition of actin, from 1.6 to 38 μM for M765 and 0.61 to 34 μM for M765NL (Table I). Thus, although M765NL displays a large decrease in actin affinity, actin is still effective in displacing ADP from the mutant myosin motor, by inducing a 56-fold weakening of ADP binding. The ratio of $\mathbf{K}_{AD}/K_D$ indicates that coupling between actin binding and ADP release is normal or slightly increased in M765NL. In contrast, the 3-fold elevated basal ATPase activity of M765NL, and the failure of actin to enhance ATPase activity to the normal extent suggest that the communication between actin- and nucleotide-binding sites is disturbed in regard to phosphate release.

In summary, deletion of 9 amino acids from the loop spanning the 50/20-kDa junction results in a myosin with almost normal nucleotide binding and hydrolysis properties but approximately 100-fold decreased actin affinity. Two independent routes of communication between the actin- and nucleotide-binding sites are apparent from this work. One route is responsible for the actin-induced phosphate release from the nucleotide-binding site. This first route of communication is disturbed by the deletion of part of loop 2. The second route, which appears to function normally in M765NL, is responsible for the actin-dependent decrease in ADP affinity that facilitates the dissociation of ADP.

Acknowledgments—We thank D. Hunt and U. Ruehl for expert technical assistance; G. Helmig and N. Adamek for preparation of actin and pyrene-labeled actin; Dr. J. Wray for critically reading the manuscript; Dr. R. Batra for critically reading the manuscript and expert assistance in designing of several experiments; Dr. M. A. Geeves for advice and helpful discussions and Dr. K. C. Holmes for continuous support and encouragement.

REFERENCES

1. Cheney, R. E., Riley, M. A., and Mooseker, M. S. (1993) *Cell Motil. Cytoskeleton* **24,** 215–223
2. Goodson, H. V., and Spudich, J. A. (1993) *Proc. Natl. Acad. Sci. U. S. A.* **90,** 659–663
3. Rayment, I., Rypniewski, W. R., Schmidt-Bäse, K., Smith, R., Tomchick, D. R., Benning, M. M., Winkelmann, D. A., Wesenberg, G., and Holden, H. M. (1993) *Science* **261,** 50–58
4. Schröder, R. R., Manstein, D. J., Jahn, W., Holden, H., Rayment, I., Holmes, K. C., and Spudich, J. A. (1993) *Nature* **364,** 171–174
5. Vikstrom, K. L., Seiler, S. H., Sohn, R. L., Strauss, M., Weiss, A., Welikson, R. E., and Leinwand, L. A. (1997) *Cell Struct. Funct.* **22,** 123–129
6. Titus, M. A.(1993) *Curr. Opin. Cell Biol.* **5,** 77–81
7. Davis, J. S.(1988) *Annu. Rev. Biophys. Biophys. Chem.* **17,** 217–239
8. Titus, M. A.(1997) *Curr. Biol.* **7,** R301–R304
9. Hasson, T., and Mooseker, M. S.(1995) *Curr. Opin. Cell Biol.* **7,** 587–594
10. Coy, D. L., and Howard, J.(1994) *Curr. Opin. Neurobiol.* **4,** 662–667
11. Mornet, D., Pantel, P., Audemard, E., and Kassab, R.(1979) *Biochem. Biophys. Res. Commun.* **89,** 925–932
12. Mornet, D., Ue, K., and Morales, M. F.(1984) *Proc. Natl. Acad. Sci. U. S. A.* **81,** 736–739
13. Kelley, C. A., and Adelstein, R. S.(1995) *Biophys. J.* **68,** 225S
14. Kurzawa-Goertz, S. E., Perreault-Micale, C. L., Trybus, K. M., Szent-Gyorgyi, A. G., and Geeves, M. A. (1998) *Biochemistry* **37,** 7517–7525
15. Uyeda, T. Q., Ruppel, K. M., and Spudich, J. A. (1994) *Nature* **368,** 567–569
16. Rovner, A. S., Freyzon, Y., and Trybus, K. M. (1995) *J. Biol. Chem.* **270,** 30260–30263
17. Furch, M., Geeves, M. A., and Manstein, D. J. (1998) *Biochemistry* **37,** 6317–6326
18. Geeves, M. A., and Conibear, P. B.(1995) *Biophys. J.* **68,** 194S-199S

19. Lehrer, S. S., and Kerwar, G. (1972) *Biochemistry* **11,** 1211–1217
20. Hiratsuka, T.(1983) *Biochim. Biophys. Acta* **724,** 496–508
21. Criddle, A. H., Geeves, M. A., and Jeffries, T.(1985) *Biochem. J.* **232,** 343–349
22. Sambrook, J., Fritsch, E. F., and Maniatis, T. (1989) *Molecular cloning: A Laboratory Manual*, Cold Spring Harbor Laboratory Press, Cold Spring Harbor, NY
23. Manstein, D. J., Schuster, H.-P., Morandini, P., and Hunt, D. M. (1995) *Gene* **162,** 129–134
24. Watts, P. J., and Ashworth, J. M. (1998) *Development* **103,** 1–16
25. Manstein, D. J., and Hunt, D. M. (1995) *J. Muscle Res. Cell Motil.* **16,** 325–332
26. Ruppel, K. M., Uyeda, T. Q. P., and Spudich, J. A.(1994) *J. Biol. Chem.* **269,** 18773–18780
27. Kurzawa, S. E., Manstein, D. J., and Geeves, M. A. (1997) *Biochemistry* **36,** 317–323
28. Millar, N. C., and Geeves, M. A. (1983) *FEBS Lett.* **160,** 141–148
29. Siemankowski, R. F., and White, H. D. (1984) *J. Biol. Chem.* **259,** 5045–5053
30. Manstein, D. J., Ruppel, K. M., and Spudich, J. A. (1989) *Science* **246,** 656–658
31. White, H. D. (1982) *Methods Enzymol.* **85,** 698–708
32. Ritchie, M. D., Geeves, M. A., Woodward, S. K., and Manstein, D. J. (1993) *Proc. Natl. Acad. Sci. U. S. A.* **90,** 8619–8623
33. Fisher, A. J., Smith, C. A., Thoden, J. B., Smith, R., Sutoh, K., Holden, H. M., and Rayment, I. (1995) *Biochemistry* **34,** 8960–8972
34. Holmes, K. C. (1997) *Curr. Biol.* **7,** R112–R118
35. Egelhoff, T. T., Manstein, D. J., and Spudich, J. A. (1990) *Dev. Biol.* **137,** 359–367
36. Patterson, B., and Spudich, J. A. (1995) *Genetics.* **140,** 505–515 37
37. De Lozanne, A., and Spudich, J. A. (1987) *Science* **236,** 1086–1091
38. Manstein, D. J., Titus, M. A., De Lozanne, A., and Spudich, J. A. (1989) *EMBO J.* **8,** 923–932